Fermi National Accelerator Laboratory

FERMILAB-Conf-88/198-E
[E-740]

Theoretical Implications of the W-Z Mass Difference and the Capabilities of the D0 Detector in Measuring It*

Rajendran Raja
Fermi National Accelerator Laboratory
P.O. Box 500, Batavia, Illinois 60510

November 1988

*Invited talk given at the 7th Topical Workshop on Proton-Antiproton Collider Physics, Fermilab, Batavia, Illinois, June 20-24, 1988.

Operated by Universities Research Association Inc. under contract with the United States Department of Energy

Theoretical Implications of the W-Z mass difference and the capabilities of the D0 detector in measuring it[1]

Rajendran Raja
Fermi National Accelerator Laboratory[2]
Batavia, Illinois, 60510, USA

November 1988

Abstract

We examine the phenomenology of the W-Z mass difference as a function of the top quark mass and the Higgs mass. A detailed analysis is presented on how well the mass difference is measurable using the D0 detector at Fermilab. We show that the effective mass distribution of the Z^0 is not a Breit-Wigner at the Tevatron and present techniques developed for the D0 detector simulation that can be used to reduce the systematic errors in measuring the W-Z mass difference. Scenarios are presented for the integrated luminosities of 10 pb^{-1} and 100 pb^{-1} at the Tevatron. It is shown that the Tevatron is competitive with LEP II for integrated luminosities of 100 pb^{-1} in attainable precisions in this measurement. These considerations argue strongly for the pp option in the Tevatron upgrade program.

[1]Invited talk given at the 7th Topical Workshop on $\bar{p}p$ collisons held at Fermilab, June 1988

[2]Fermilab is operated by the Universities Research Association Inc. under contract with the U.S Department of Energy

Phenomenology of radiative corrections in the electroweak theory

In what follows, we adopt the definition of the weak mixing angle due to Sirlin [1].

$$sin^2\theta_W \equiv 1 - \frac{M_W^2}{M_Z^2} \tag{1}$$

This implies

$$M_Z^2 \equiv \frac{M_W^2}{cos^2\theta_W} \tag{2}$$

From low energy phenomenology, one can show [2] that

$$M_W^2 = \frac{A^2}{(1-\Delta r)sin^2\theta_W} \tag{3}$$

where

$$A = \sqrt{\frac{\pi\alpha}{\sqrt{(2)}G_\mu}} = 37.281 \pm 0.003GeV \tag{4}$$

with the muon decay constant $G_\mu = 1.16634 \pm 0.00002 \times 10^{-5}GeV^{-2}$ with the inverse fine structure constant $1/\alpha = 137.035963(15)$. Δr is the term due to radiative corrections at the one loop level in the electroweak theory. Figure (1) shows the source of relevant one loop diagrams which determine the W and Z self energies (masses). It can be seen that Δr is a function of the top quark mass and the Higgs mass, the two unknown masses in the theory. Note that in this formalism,

$$\rho \equiv \frac{M_W^2}{M_Z^2 cos^2\theta_W} \equiv 1 \tag{5}$$

by definition, within the standard model. We will only need to consider models with $\rho \neq 1$ if the standard model is found to be inconsistent by measuring the W-Z mass difference. There are thus four unknowns M_W, M_Z, $sin^2\theta_W$, and Δr and two equations 2 , 3. So one can express everything in terms of two variables which we can choose to be M_Z and Δr. Δr depends on the Higgs mass and the top quark mass as stated previously. It also depends on other fermion masses such as the charm quark mass, bottom quark mass etc, but these masses are constrained from low energy phenomenology.

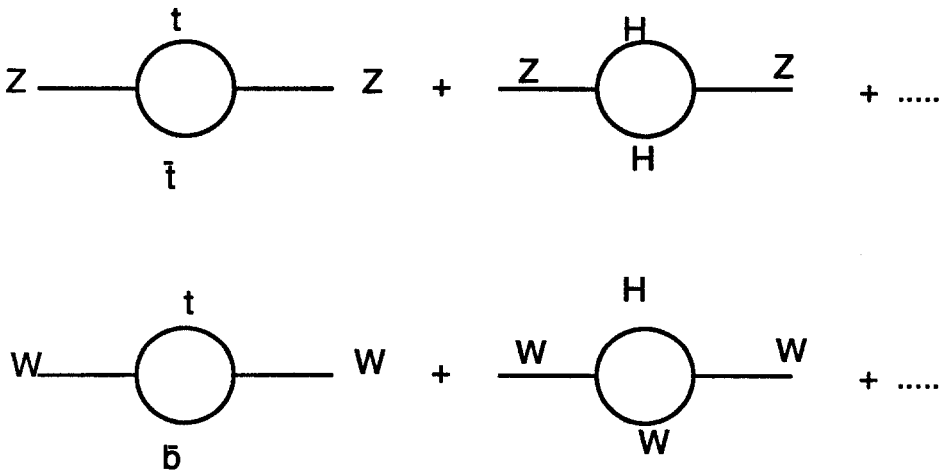

Figure 1: One loop diagrams for W and Z self-energies

Note that

$$M_W^2 = \frac{\pi}{\sqrt{(2)}G_\mu}\frac{\alpha}{1-\Delta r}(sin^2\theta_W)^{-1} \tag{6}$$

$\alpha/(1-\Delta r)$ can be re-interpreted as $\alpha(M_W^2)$, the value of the QED running coupling constant at $Q^2 = -M_W^2$ [3]. If we assume that $M_{Higgs} = M_Z$, $m_c = 1.5\ \ GeV/c^2$, $m_b = 4.5\ \ GeV/c^2$ and $m_t = 36\ \ GeV/c^2$ [4], we get $\Delta r = 0.0696 \pm 0.0020$. This leads to "predictions" of the W and Z masses of $M_W = 83.0 + 2.9 - 2.7\ \ GeV/c^2$ and $M_Z = 93.8 + 2.4 - 2.2\ \ GeV/c^2$. Note that these numbers assume a value for the top quark mass which may not be realistic. However, if $\Delta r = 0$, $M_W = 78.2\ \ GeV/c^2$ which is well outside the measured values by UA1 and UA2 [5]. This indicates that radiative corrections are important and need to be taken into account while calculating masses in the electroweak theory [2]. Note also that $\alpha(M_W^2) = 1/127.5$ i.e the QED coupling constant increases for larger Q^2. This is the opposite of the QCD asymptotic freedom situation.

In what follows, we treat Δr as a function of m_t and m_H, the top quark and Higgs masses respectively. So one can make tables of M_W and $sin^2\theta_W$ for various values of M_Z, m_t and m_H [6] [7]. LEP will soon measure M_Z accu-

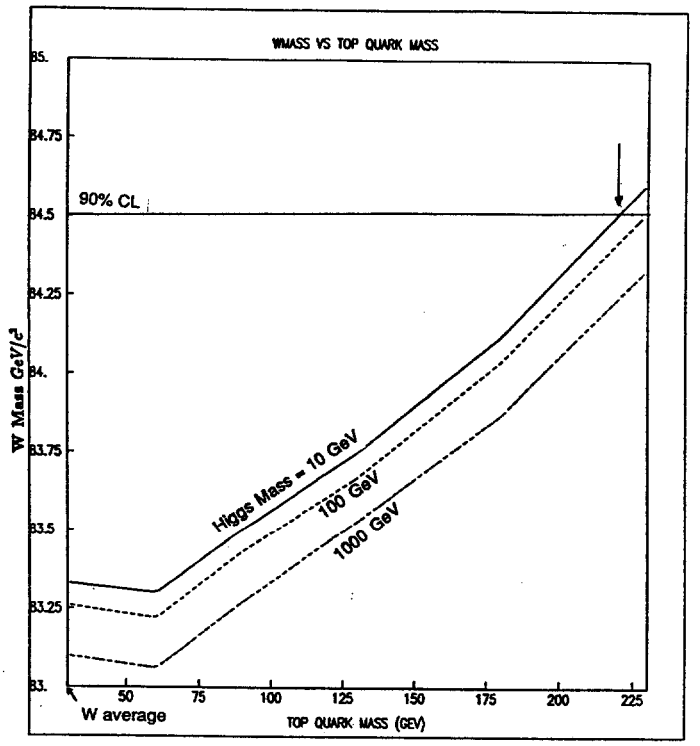

Figure 2: Variation of the W mass as a function of the top quark mass. $M_Z = 94.0\ GeV/c^2$

rately. According to Altarelli [8], $\Delta M_Z = \pm 30 MeV/c^2$ should well be within the reach of LEP once QED radiative corrections are taken into account. We assume conservatively that the Z mass is measurable to an accuracy of $\pm 50 MeV/c^2$ by the time the Tevatron measurements of the W-Z mass difference is preformed.

For the rest of this analysis, we will assume that LEP has measured $M_Z = 94.0 \pm 0.050\ GeV/c^2$. Once the true value of M_Z is known, it should be easy to scale up the curves presented here with minor changes in the conclusions.

Figure (2) shows the variation of the W-Z mass difference [6] as a function of the top quark mass. The three curves are for Higgs masses of 10 , 100 and 100 GeV/c^2. The reason the curves are not quite smooth is due to truncation errors in the data which were published as numerical tables. It can be seen that as the top quark mass varies from 50 GeV/c^2 to 225 GeV/c^2 , the W mass changes from $\sim 83.5\ GeV/c^2$ to $\sim 84.3\ GeV/c^2$. The W mass is a weak function of the Higgs mass.

Table 1 shows the published UA1/UA2 data on W and Z masses . [5].

	$UA1\ data(\ GeV/c^2)$	$UA2\ data(\ GeV/c^2)$
M_W	$82.7 \pm 1.0 \pm 2.7(syst.)$	$80.2 \pm 0.6 \pm 0.5(syst1.)$ $\pm 1.3(syst2.)$
M_Z	$93.1 \pm 1.0 \pm 3.1(syst.)$	$91.5 \pm 1.2 \pm 1.7(syst.)$
M_W *scaled to Z mass*	83.5 ± 1.35	82.4 ± 1.24
M_W *scaled* $(UA1, UA2\ average)$	82.95 ± 0.92	$< 84.5\ at\ 90\%\ CL$

Table 1: UA1 and UA2 data on W and Z masses scaled to Z mass of 94.0 GeV/c^2

Scaling up the Z mass to 94.0 GeV/c^2 and averaging, one gets $M_W = 82.95 \pm 0.92\ GeV/c^2$. i.e. $M_W < 84.5\ GeV/c^2$ at 90% confidence level. From figure 2 this implies that $m_t < 225\ GeV/c^2$ for $m_H = 10\ GeV/c^2$ and $m_t < 230\ GeV/c^2$ for $M_H = 1000\ GeV/c^2$. This analysis can be honed further by including low energy data as well yielding a slightly tighter limit of $m_t < 180\ GeV/c^2$ [9].

Fitting Techniques

Because of the fundamental importance of the measurement and the need to hold down systematic differences between the determination of M_W and M_Z, careful attention needs to be paid to fitting techniques. Since electrons are measured with greater precision than muons in current collider experiments, we will only consider the channels $Z \rightarrow e^+e^-$ and $W \rightarrow e\nu$ in what follows. For the Z channel, we can fit the full effective mass distribution since both final state particles are measured. For the W, only the transverse momentum of the neutrino is measured (inferred from the transverse momentum of the underlying event and that of the electron). The longitudinal momentum of the neutrino is unmeasurable due to the loss of particles down the beam pipe. The statistical accuracy of the W mass fit is governed by the number of events populating the Jacobian edge of the transverse mass distribution. The number of $Z \rightarrow e^+e^-$ events is lower than the number of $W \rightarrow e\nu$ events

by $\sim$ a factor of 10. However, the number of W's in the falling edge of the transverse mass distribution is roughly a tenth of the total number of W decays. The numbers thus conspire to give both measurements roughly the same statistical accuracy. The Z mass is however not sensitive to the hadronic energy measurement of the event. The W transverse mass measurement, on the other hand, is sensitive to the measurement of the hadronic energy in the event since p_t of the W and the E_T of the neutrino is inferred from the p_t of the underlying event.

If one has large statistics, one can drop one of the electrons in the Z decay and treat the Z fit in exactly the same fashion as the W fit. i.e. fit the transverse mass of the Z. This results in a loss in statistical precision of the Z mass measurement but is accompanied by a simultaneous gain on the systematic error front since both the Z and the W are now treated identically. In what follows we will explore techniques aimed at understanding the hadronic sector better and leave the above option as a cross check.

Withe 10 pb^{-1} at the Tevatron, we expect $\sim 15,000\ W \rightarrow e\nu$ events and $\sim 1500\ Z \rightarrow e^+e^-$ events before cuts. In this analysis we will present errors based on 10,000 W's and 1,000 Z's.

Fitting for the Z mass

We show that the effective mass of the Z is <u>not</u> distributed as a simple Breit-Wigner. The reason for this is that the parton luminosities are larger , the smaller the effective mass of the Z. So the lower mass Z's are formed preferentially in greater numbers than the higher mass ones resulting in a skewed Breit-Wigner.

With $\tau = M^2/s$ where M is the effective mass of the Z (not the Central value), and s is the center of mass energy squared, we can write , using the parton fusion model

$$\frac{x d^2\sigma_Z}{dx d\tau} = \sum_q (q(x)\overline{q}(\tau/x) + q(\tau/x)\overline{q}(x)) BW(M^2) \tag{7}$$

where $q(x)$ is the probability distribution function of the quark species q in the proton and $\overline{q}(x)$ is the corresponding distribution in the anti-proton,

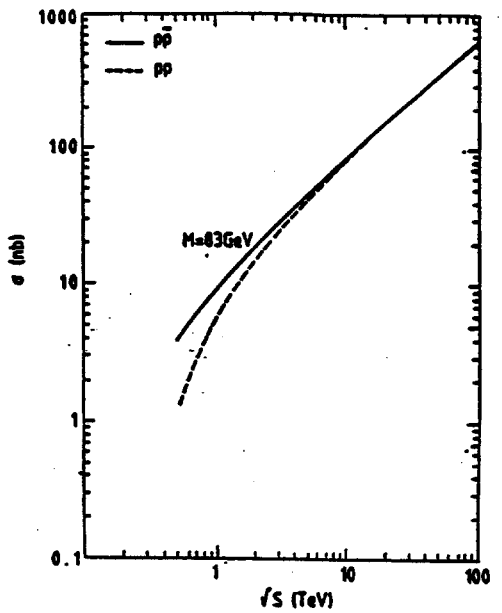

Figure 3: s dependence of the W cross section

BW(M^2) is the Breit-Wigner distribution . Integrating over x, one gets

$$\frac{d\sigma_Z}{dM^2} = \frac{1}{s}\sum_q \int_{x=\tau}^{x=1} (q(x)\overline{q}(\tau/x) + q(\tau/x)\overline{q}(x)\frac{dx}{x})BW(M^2) \tag{8}$$

Integrating [10] over M^2 and assuming a narrow Breit-Wigner, one gets

$$\sigma_Z(\frac{M_Z^2}{s}) = \tau\sum_q \int_{x=\tau}^{x=1} (q(x)\overline{q}(\tau/x) + q(\tau/x)\overline{q}(x)\frac{dx}{x})\lambda \tag{9}$$

where λ is a constant and τ is now M_Z^2/s with M_Z the central Z mass. This immediately suggests a method of determining the skewing function of the Breit-Wigner. Either one can work it out directly from the structure functions, or one can determine it by studying the energy dependence of the Z cross section. The latter method should be employed in practice, since that is directly linked to the data. Figure 3 is the calculated s dependence of the W cross section [11]. For purposes of estimating the structure function effect, we assume that the Z cross section energy dependence is the same as the W cross section energy dependence. For the region of interest of τ, we

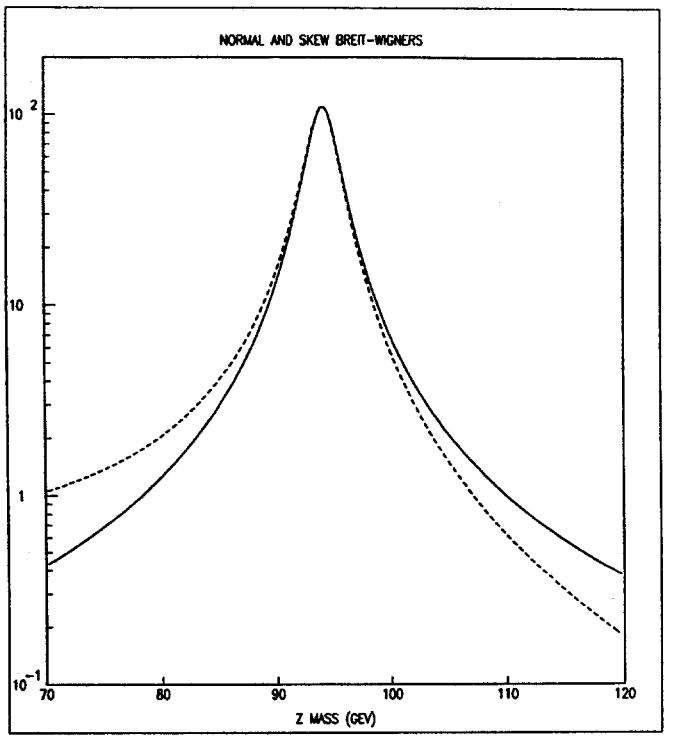

Figure 4: Effective mass distribution for $M_Z = 94 \ GeV/c^2$. Skewed and unskewed Breit-Wigners

can parametrize the cross section as being linear in $\sqrt{(s)}$. i.e.

$$\sigma = \frac{A}{\sqrt{(\tau)}} + B \tag{10}$$

This implies that the structure function variation across the Breit Wigner is $(A/\sqrt{(\tau)} + B)/\tau$ where τ is now M^2/s. We normalize the skewing function so that at the central Z mass, M_Z, the skewing factor is unity. Since B is small, the net variation is roughly independent of s and only depends on M^2. i.e. the skewing effect is roughly the same magnitude at both CERN and Fermilab energies. Figure 4 is the skewed Breit-Wigner and the unskewed Breit-Wigner shape superimposed on each other and normalized to 1000 Z's. The mean of the skewed Breit-Wigner is at 93.22 GeV/c^2.i.e. there is a shift of 780 MeV downward . This shift is clearly a function of how many Z's one has in the sample since the amount of tail one builds up will affect the net shift down. As one adds more statistics, the skewing effect will become more pronounced. One thus concludes that it is important to take into account the structure function variation and the effect is best determined experimentally

by measuring the Z and W cross sections as a function of energy. Both UA1 and UA2 fit the Z presently using an unskewed Breit Wigner. This will have to be altered as more statistics are generated.

To summarize,

- It is necessary to generate the full skewed Breit-Wigner shape for a grid of mass and width combinations for the Z to fit for the Z mass.
- One can generate the likelihood curves by using the measured set of Z 3 vectors in conjunction with the underlying event and varying the mass and width of the Z along a discrete grid of points.
- The electron pairs thus generated should be put through a full simulation of the detector response.
- The goodness of fit for each grid point of mass and width can be determined either by maximum likelihood or by such tests as the Kolmogorov test.
- The most likely mass and width of the fit can be determined by interpolation in the likelihood surface in the mass-width space.
- with 1000 Z's , we believe it is possible to achieve a statistical accuracy of $\pm 120 MeV/c^2$ for the Z mass.
- We use the Z mass obtained thus to provide the absolute calibration for the detector . We re-adjust our energy scale so that Z mass agrees with the LEP value. This would then remove the first order energy scale error in the W-Z mass difference.

W mass fitting technique

The W transverse mass , m_T is defined as

$$m_T^2 = 2E_T^{\nu} E_T^{e}(1 - cos\phi^{e\nu}) \tag{11}$$

where $E_T^{e,\nu}$ are the transverse energies of the leptons and $\phi^{e\nu}$ is the angle in the transverse plane between the two leptons.

Transverse mass is the best variable to fit for the W mass since it is relatively insensitive to errors made in measuring the transverse momentum of the W[12]. The likelihood curves are generated for a grid of mass and width points. This time the generation and detector simulation of the underlying event is crucial since the information on the W p_T is contained therin. One can take two separate approaches.

- Generate the full event using an event generator such as Isajet [13]. Take the full event through the detector simulation. See next section on detector simulation techniques that make this possible. This method relies on Isajet getting the details of the underlying event correct.

- Alternatively, use the measured electron and p_T^W to solve for the neutrino 4 Vector. Resolve the two-fold ambiguity in the quadratic solution for the neutrino longitudinal momentum by choosing the solution with the smallest Feynman x for the W. One can then use the W three momentum and the experimentally obtained underlying event to generate a set of W decays for a grid of M_W, Γ_W. This can be done for the entire W sample. A single event can be used to generate many fake decays for the likelihood curves. This technique economizes computer time since there is no need to simulate the rest of the event. One merely needs to put the electron though the detector simulation. However, the arbitrary resolution of the neutrino ambiguity may be a source of systematics, although such systematics are easily estimated and corrected for.

Figure 5 is a typical transverse mass distribution obtainable for a 10 pb^{-1} run of data with the D0 detector for a W of mass 83 GeV/c^2 and width 3 GeV/c^2. Figure 6 is a set of likelihood curves for W masses varying between 75 GeV/c^2 and 90 GeV/c^2 in steps of 1 GeV/c^2 for a W width of 3.0 GeV/c^2. We emphasize that the full detector simulation has not been done for these curves. The particle 4 Vectors have merely been smeared by the expected resolutions ($15\%/\sqrt{(E)}$ and a 2% constant term in quadrature for electrons and $50\%/\sqrt{(E)}$ and 5% constant term in quadrature for hadrons .)

Figure 7 shows a set of likelihood curves for W mass of 83 GeV/c^2 with the width varying between 0 GeV/c^2 and 7.5 GeV/c^2 in steps of 0.5 GeV/c^2. Figure 8 is the negative log likelihood surface obtained for a typical fit. Using

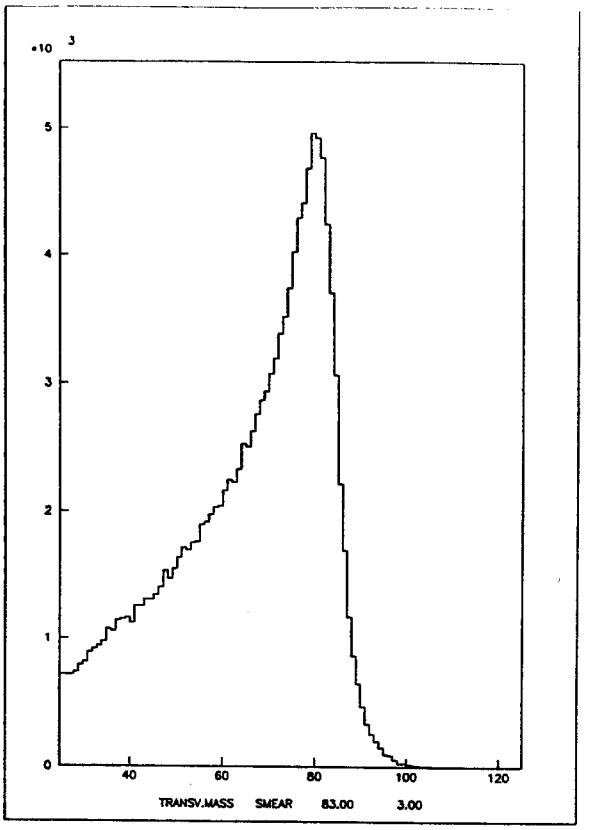

Figure 5: Transverse mass distribution for $M_W = 83\ GeV/c^2$ and width = 3 GeV/c^2 smeared by experimental resolution

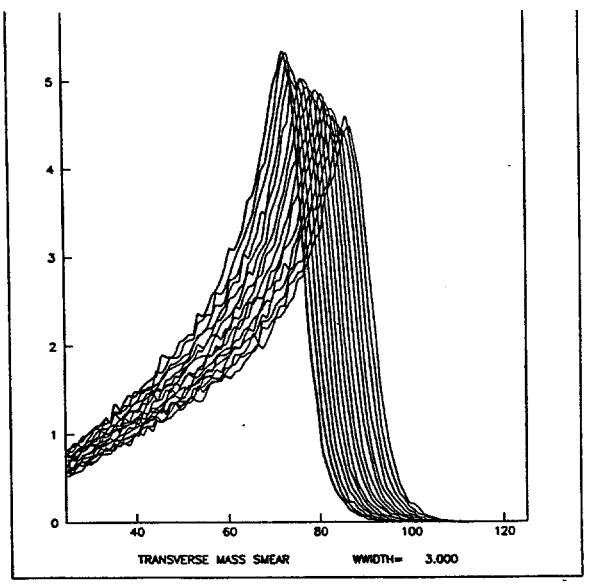

Figure 6: Likelihood curves for fitting the W transverse mass. M_W varies from 75 GeV/c^2 to 90 GeV/c^2 in steps of 1 GeV/c^2. Width of the W is fixed at 3 GeV/c^2 for these curves

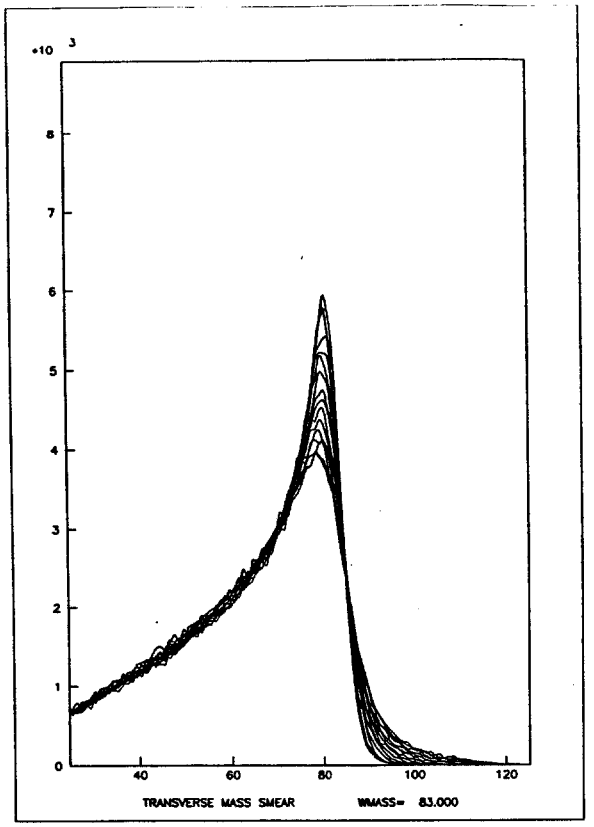

Figure 7: Likelihood curves for fitting the W transverse mass. Γ_W varies from 0 GeV/c^2 to 7.5 GeV/c^2 in steps of 0.5 GeV/c^2. M_W is fixed at 83 GeV/c^2 for these curves

cubic spline interpolation, one can find the minimum of the surface and obtain the 1σ and the 2σ contours. Figure 9 is a typical result. There is a slight correlation between the mass and the width of the W resulting from the fact that we are fitting the edge of the Jacobian peak for both the mass and the width information. Smaller mass values can be compensated for by going to larger widths. For 10 pb^{-1} of data, we expect typical statistical mass errors of $\delta M = \pm 200 MeV/c^2$ and width errors of $\pm 250 MeV/c^2$. In order to hold down the systematics in the W fit, it is necessary to simulate the hadronic sector of the event well. This means simulating the calorimeter in some detail including cracks and dead material. Figure 10 shows the D0 Monte Carlo picture of the calorimeter with cryostat and other dead material shown. The main problem with hadronic simulations in the past is that parametrizations of showers have been used to simulate hadronic energy deposition. These parametrizations do not take into account correlations within the shower well and have difficulty accomodating dead material effects and cracks. In D0, we employ the full Gheisha shower simulation [14] and the Geant package [15]. Figure 11 shows the D0 simulation of showers, both

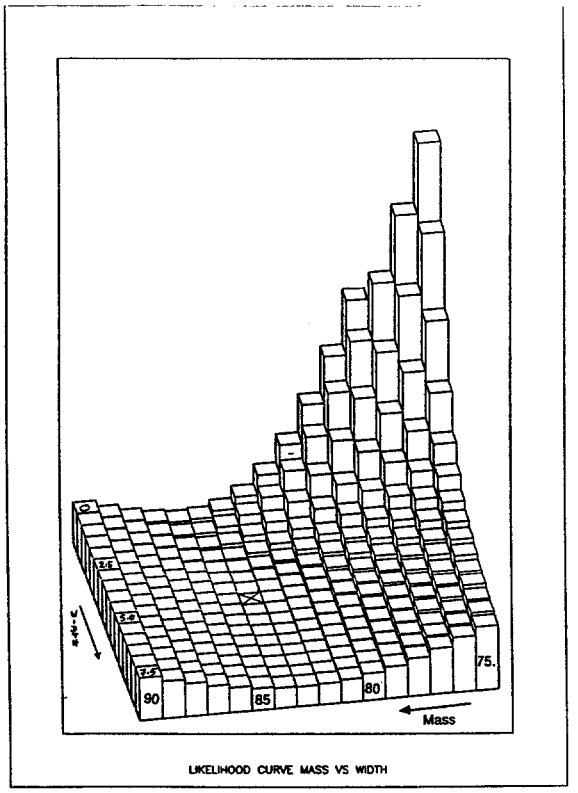

Figure 8: Likelihood surface for W fit. Mass and width vary along a grid of points

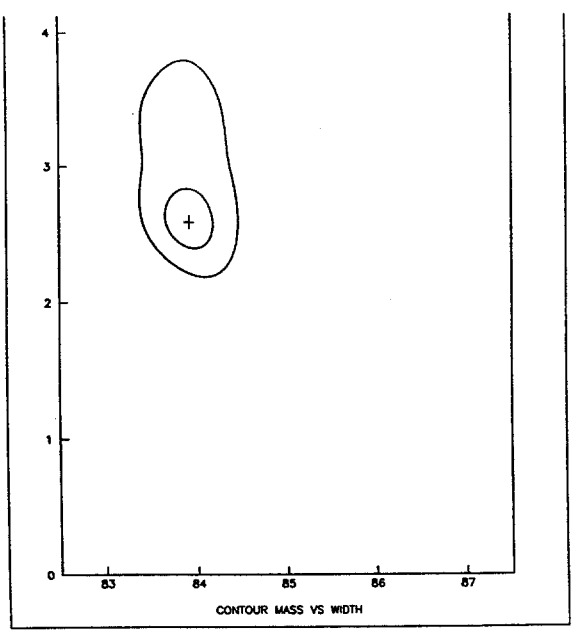

Figure 9: 1 sigma and 2 Sigma contours on the likelihood surface found by interpolation

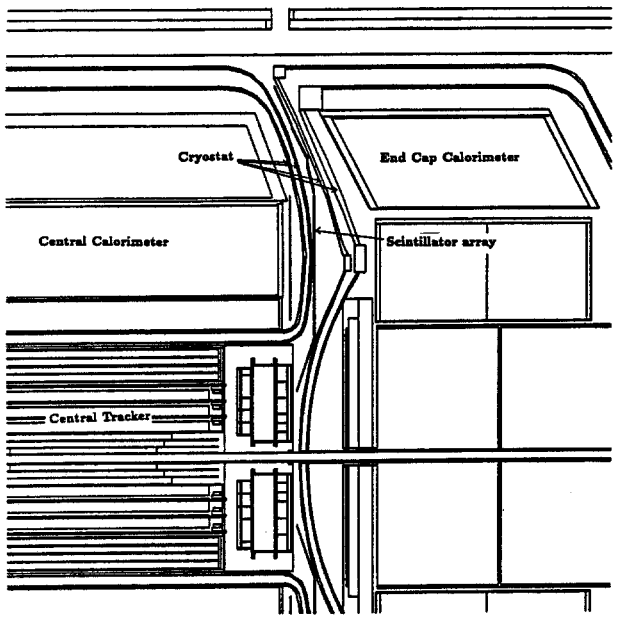

Figure 10: Detail of the GEANT simulation of the D0 detector

electromagnetic and hadronic in some detail. These showers take into account correlations, dead material effects and cracks correctly. However, they take a great deal of computing time to generate. To generate one full two jet event at Tevatron energies, one needs typically 3 CPU hours of VAX 780 time. We have used a microvax farm of computers to simulate 10,000 Isajet events through D0GEANT. The output was saved shower by shower and used to generate a random access library of showers [16]. These showers can be re-used to simulate other events with accompanying factor of 60 speed up in computing time. We plan to use this technique, invented for D0, to simulate the hadronic sector of W events. Dead material and crack effects are handled correctly by the shower library technique.

$10pb^{-1}$ scenario at the Tevatron

Figure 12 shows the discovery limit as a function of integrated luminosity for CERN and Fermilab energies. The discovery limit is defined for the purposes of this discussion as that top quark mass at which 100 $t\bar{t}$ events are produced in the experiment. We only use the $t\bar{t}$ channel for this argument and neglect

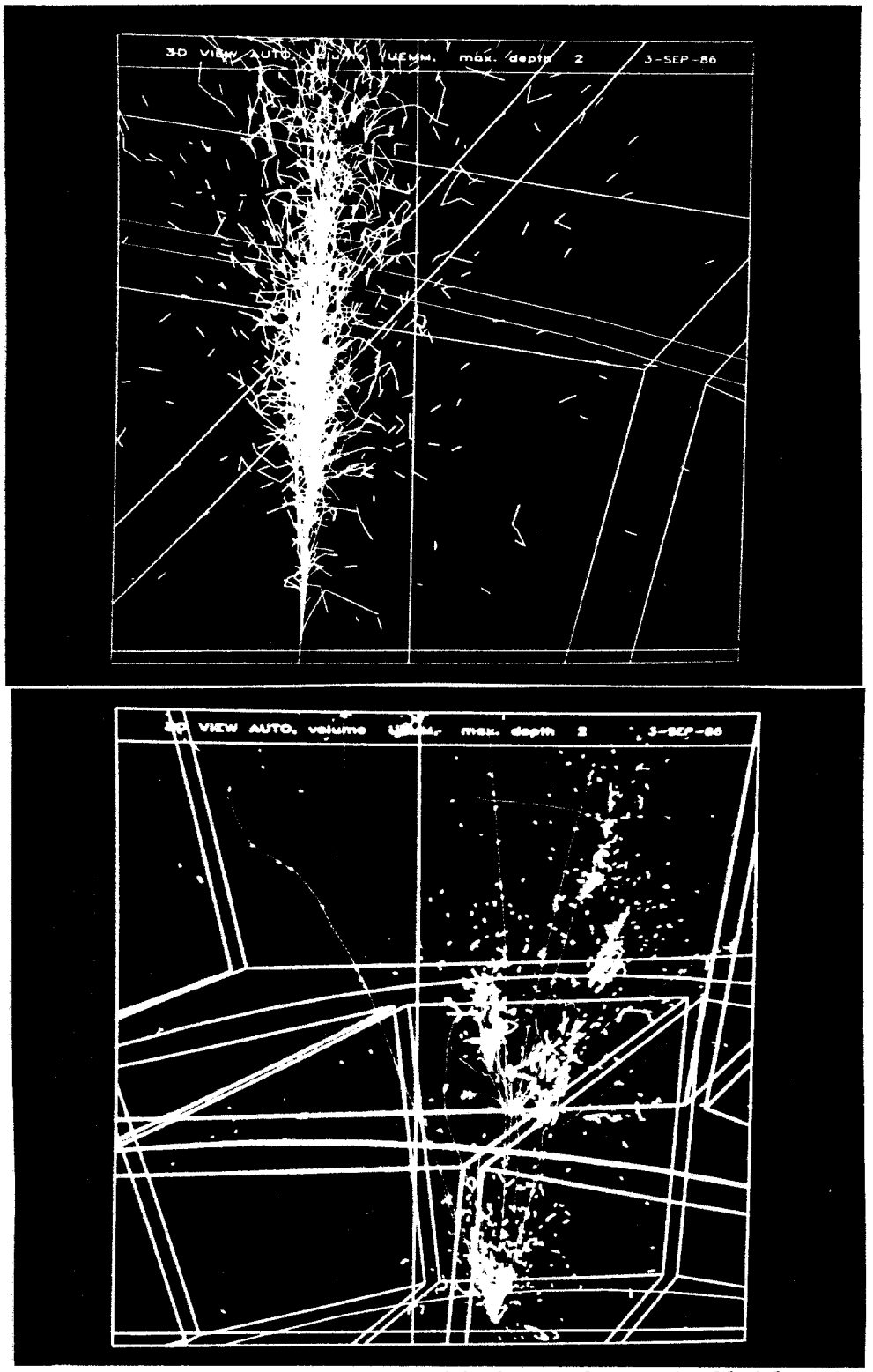

Figure 11: Electromagnetic and hadronic showers in Gheisha

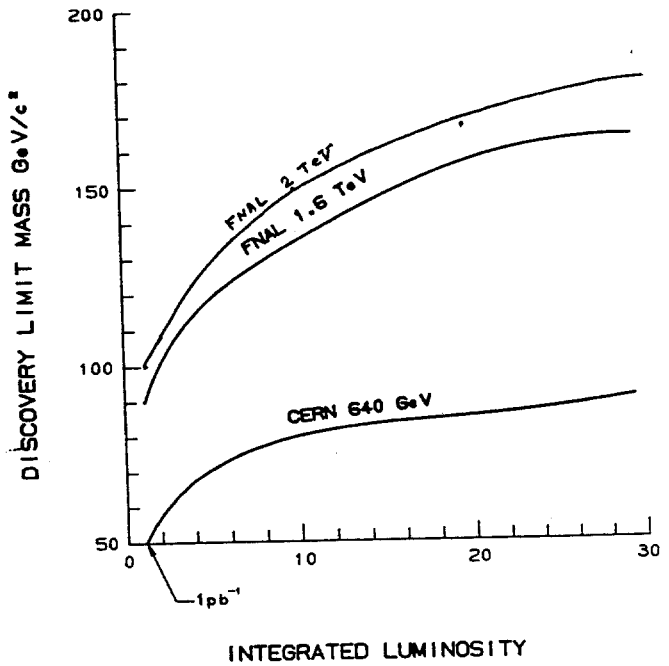

Figure 12: Discovery limit of the top quark as a function of integrated luminosity

the $W \rightarrow t\bar{b}$ which is significant only for a limited mass range of top quark (40 GeV/c^2 - $\sim$ 65 GeV/c^2). It can be seen that for 10 pb^{-1} of integrated luminosity, CERN can see a top quark if it is below 80 GeV/c^2 and Fermilab at 1.8 TeV will see it if it is below 140 GeV/c^2. If one insists on having say, 200 $t\bar{t}$ events before the top is discoverable, then this shifts the discovery limit down by $\sim$ 10 GeV/c^2. Figure 13 shows two possible scenarios. If the top quark mass is below 140 GeV/c^2, the lower scenario for the W mass will hold with the indicated errors. The W-Z mass difference measurement can be used to set constraints on the top quark mass and help search for it in the data. If however, it is greater than 140 GeV/c^2, the upper scenario for the W mass will hold and the measurement again can be used to predict the top quark mass. The search for the top quark and the W-Z mass difference measurement should go on concomitantly.

100 pb^{-1} scenario at the Tevatron

We now consider the $100pb^{-1}$ scenario with a Tevatron upgrade. With a pp machine at a luminosity of 10^{32}, 11 days of running will produce 100,000

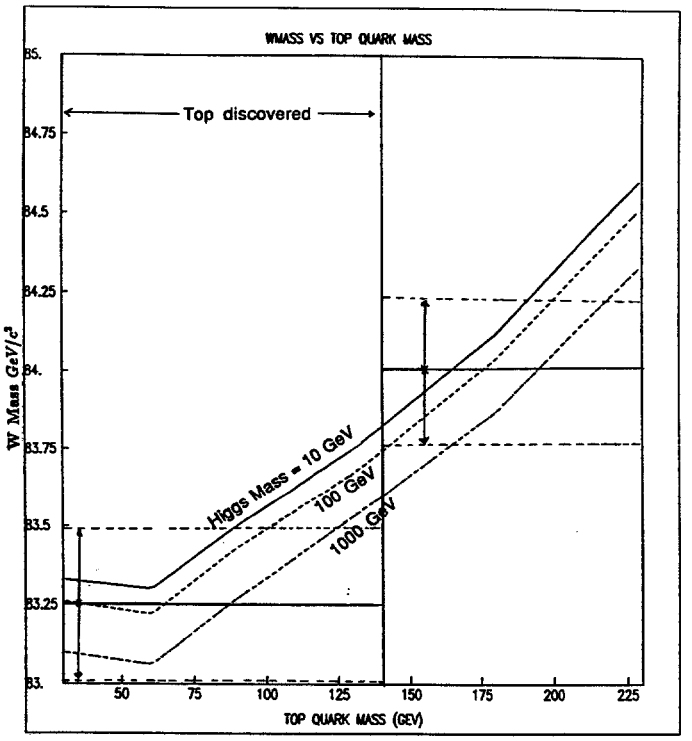

Figure 13: 10 pb^{-1} scenario at the Tevatron

W's and 10,000 Z's. δM_W can be measured to ± 0.075 GeV/c^2 statistically. We assume that the techniques outlined above can be used to control the systametics to the required accuracy. The Z transverse mass can now also be fitted by dropping one of the electrons. There is enough statistics and this gives another handle on systematics. Figure 14 shows a possible scenario. The top quark discovery limit is now 240 GeV/c^2 and a standard model top quark must be discovered. We assume that such a top quark has been discovered and its mass determined accurately using the Tevatron, LEP II or a new genration of e^+e^- collider. If this is the case, then the precision measurement of the W-Z mass difference will enable one to get an idea of the Higgs mass. It will provide a crucial test of the standard model. If discrepancies are found, a whole host of scenarios can be invoked outside the standard model to explain the data. Table 2 shows the shift in the W mass due to scenarios such as the fourth generation, heavy lepton pairs, SUSY and Technicolor. It can be seen that the limits obtained on the top quark mass earlier assume the completeness of the standard model. It is possible to have a very heavy top quark which will drive the W mass up, and technicolor which will drive the W mass down again to the observed value. In general

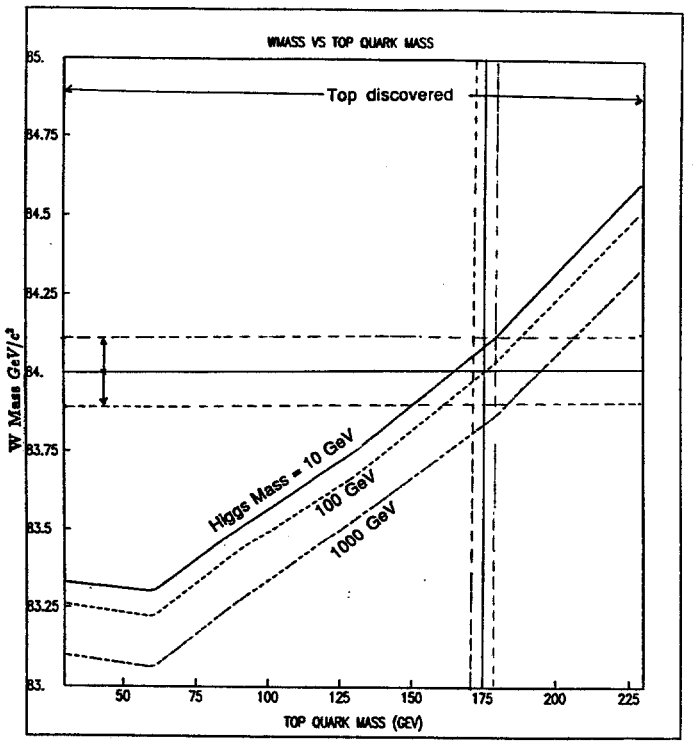

Figure 14: 100 pb^{-1} scenario at the Tevatron

fermion pairs with large splitting will drive the W mass up whereas, existence of scalars such as in Technicolor will drive the W mass down.

To conclude, the D0 detector with the high luminosity pp upgrade option, with its liquid argon calorimetry providing stable calibration, provides a tool for measuring the W-Z mass difference to a precision comparable to what is obtainable elsewhere [17]. The measurement in the 10 pb^{-1} scenario can help predict the top quark mass if it is greater than 140 GeV/c^2 and in the 100 pb^{-1} scenario can help establish the completeness or otherwise of the standard model.

	$\delta M_W(MeV)$
New Heavy quark pair	
Large splitting	300
Degenerate	-42
Heavy Lepton pair	
Large splitting $m_\nu = 0$	300
Degenerate	-14
Heavy squark pair, slepton pair	
Large splitting	300
Degenerate	0
Winos	
$m_{3/2} \ll 100\ GeV/c^2$	100
$m_{3/2} \gg 100\ GeV/c^2$	< 10
Technicolor	
$SU_8 X SU_8$	-500
O_{16}	-500

Table 2: Shift in the W mass due to effects beyond the standard model

References

[1] A. Sirlin, Phys. Rev D22 ,971 (1980).

[2] W.J.Marciano and A.Sirlin, Phys. Rev. D22, 2695 (1980)
A.Sirlin and W.J.Marciano, Nucl. Phys. B189, 442 (1981)
Testing the standard model by precise determinations of $W^{\pm}$ and Z masses, W.J.Marciano and A.Sirlin, Phys Rev D29, 945. (1984)

[3] W.J.Marciano, Phys. Rev D20, 274 (1979)
W.J.Marciano and A. Sirlin Phys. Rev. Lett. 46, 163 (1981)
A.Sirlin, Phys. Rev. D29, 89 (1984)

[4] W. Wetzel, Z. Phys. C 11 , 117 (1981)
W. Marciano, Aspen Winter Conference 1985.
M. Consoli, S. Lo Presti and L. Maiani, Nucl. Phys. B 223, 474 (1983)

[5] UA1 data used for this analysis is from the presentations at the Uppsala Conference (1987)
UA2 data come from CERN-EP87-05.

[6] B.W. Lynn, M.E.Peskin and R.G.Stuart, Physics at LEP (J.Ellis, R.Peccei, editors) Vol 1, Cern 86-02, Page 90.

[7] B.W.Lynn and R.G.Stuart, Nucl. Phys. B 253,216 (1985)

[8] G. Altarelli et. al. Physics at LEP (J.Ellis, R.Peccei, editors) Vol 1, Cern 86-02, Page 1.

[9] A comprehensive analysis of data pertaining to the weak neutral current and the intermediate vector boson masses. U. Amaldi et.al, Phys.Rev.D36:1385,1987.

[10] Physics at $\sqrt{s}$ = 2 TeV, an Experimenter's Perspective, R.Raja, Fermilab-PuB 87/125-E. See derivation of these formulas therein.

[11] G. Altarelli, R.K. Ellis, and G. Martinelli, Z.Phys. C27, 617 (1985).

[12] The transverse mass and width of the W boson. J. Smith, W.L. van Neerven, J.A.M. Vermaseren ,Phys.Rev.Lett.50,1738(1983).

[13] ISAJET v. 5.22, A Montecarlo Event Generator for $\bar{p}p$ and pp Interactions, F.E. Paige and S.D. Protopopescu, BNL-38034

[14] Gheisha is a hadronic shower generator program written by H. Fesefeldt.

[15] User's Guide to GEANT 3.10, R.Brun et al, CERN DD-EE-84-1

[16] On Micro Vax farms and Shower libraries - Monte Carlo techniques developed for the D0 detector, R.Raja, Proceedings of the 1987 Workshop on SSC detector Simulation, Argonne National Laboratory.

[17] G. Barbiellini et. al. Physics at LEP (J.Ellis, R.Peccei, editors) Vol 2, Cern 86-02, Page 1.